

Axial Nanometer Distances Measured by Fluorescence Lifetime Imaging Microscopy

Michael Berndt,[†] Mike Lorenz,[†] Jörg Enderlein,[‡] and Stefan Diez^{*†}

[†]Max-Planck-Institute of Molecular Cell Biology and Genetics, 01307 Dresden, Germany, and [‡]III. Institute of Physics, Georg-August-University, 37077 Göttingen, Germany

ABSTRACT We present a novel fluorescence lifetime imaging microscopy technique to measure absolute positions of fluorescent molecules within 100 nm above a metalized surface based on distance-dependent fluorescence lifetime modulations. We apply this technique to fluorescently labeled microtubules as optical probes with various unlabeled proteins attached. By measuring the fluorescence lifetimes, we obtain the position of the microtubules and therefore determine the geometrical size of the attached proteins with nanometer precision.

KEYWORDS Absolute distance measurement, fluorescence lifetime, FLIM, microtubules, avidin, neutravidin, kinesin-1

The design of innovative applications in the field of bionanotechnology requires tools capable of measuring molecular parameters under ambient conditions. Therefore, a number of techniques to localize fluorescent molecules in the lateral dimension (i.e., parallel to a substrate surface) with nanometer accuracy have been recently developed.¹ However, performing this task in the axial dimension (i.e., perpendicular to a substrate surface) is still challenging.

So far, techniques which have been used to address this issue of *absolute* axial localization are: (i) total-internal reflection fluorescence (TIRF) microscopy,² using evanescent fields to axially localize single particles³ and (ii) fluorescence interference-contrast (FLIC) microscopy⁴ which axially localizes molecules in an interferometric way.⁵ While both techniques offer a much higher accuracy than the diffraction limit of light, they are susceptible to intrinsic spatial and temporal intensity fluctuations, such as inhomogeneous labeling and excitation, as well as photobleaching; because in both cases the measured intensity values are directly converted into axial distances.

To overcome these limitations, we developed a novel method to determine the axial position of fluorescently labeled molecules above a surface. We make use of the decrease in fluorescence lifetime of a fluorescing molecule when brought into the vicinity of a metal surface. This effect is based on the physical principle of strong optical near-field coupling that occurs in proximity to metals. The lifetime modulation is nonlinearly dependent on the distance from the metal surface and is quantitatively well described.⁶ The lifetime of single fluorophores in direct contact to the metal surface is zero and increases nonlinearly with increasing

distance of the fluorophore from the surface until it reaches asymptotically the lifetime value of a free fluorophore (i.e., without presence of a surface). Hence, fluorescence lifetime can be used to axially localize fluorescing molecules up to 100 nm above a surface with high accuracy. To demonstrate the technique, we use fluorescently labeled microtubules as rigid and straight probes.⁷ Microtubules, which form a large part of the cytoskeleton found in eukaryotes, are hollow tubular structures composed of the globular protein tubulin. They have a typical length of several tens of micrometers and an axial geometry of about 25 nm in diameter, known from EM studies.⁸ They can be easily reconstituted *in vitro*,⁹ where they are composed of mostly 13–15 protofilaments, changing their diameter negligibly for our purpose.¹⁰ We mount Alexa Fluor 488 labeled microtubules at various distances above a 15 nm flat gold surface by attaching microtubule-associated (kinesin-1) and non-microtubule-associated (avidin and neutravidin) proteins to their lattice and measure their fluorescence lifetime with fluorescence lifetime imaging microscopy (FLIM) (Figure 1). Thereby, we are able to image and determine the absolute axial elevation of the microtubules and hence the geometrical size of the attached proteins (see Supporting Methods in the Supporting Information).

A schematic of the different experiments with corresponding lifetime images is shown in Figure 2. In Figure 2a microtubules are fixed to the surface by an avidin layer. In Figure 2b neutravidin is additionally bound via biotin to the microtubules before surface fixation by avidin. In Figure 2c microtubules are held by kinesin-1 motor proteins. The obtained fluorescent lifetimes are clearly different in all three experiments (see Supporting Discussion in the Supporting Information for details). The mean lifetime of the microtubules fixed by avidin to the gold surface is 0.91 ± 0.05 ns (standard error of the mean (s.e.m.), $n = 24$ regions from various samples) (Figure 2a). This value is smaller than the

* Corresponding author: tel, +49-351-210-2521; fax, +49-351-210-2020; e-mail, diez@mpi-cbg.de.

Received for review: 02/18/2010

Published on Web: 03/10/2010

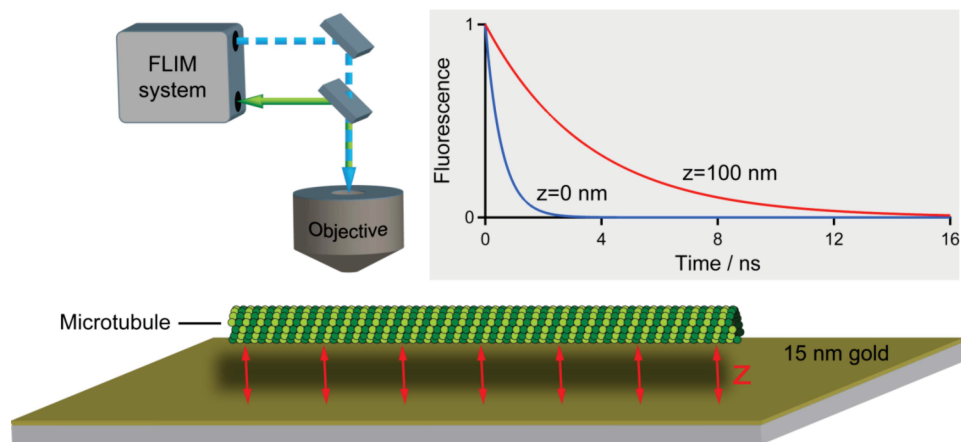


FIGURE 1. Schematic diagram of the experimental setup. Fluorescently labeled microtubules are elevated via different spacer molecules (not shown) at axial distances above a 15 nm gold surface in a microscope flow cell. Fluorescent lifetimes, measured with a FLIM system (example exponential decays for two different distances z shown on the upper right) are used to obtain and image the axial position of the microtubules with nanometer exactness.

mean lifetime of the microtubules additionally coated with neutravidin 1.21 ± 0.08 ns ($n = 5$) (Figure 2b), or the lifetime of the microtubule–kinesin system, 1.87 ± 0.04 ns ($n = 16$) (Figure 2c). In comparison the unperturbed lifetime of Alexa Fluor 488 labeled microtubules in free solution (i.e., $\gg 100$ nm above the surface) is measured to 3.53 ± 0.05 ns ($n = 5$). This is independently verified by measuring the quantum yield of the Alexa Fluor 488 labeled microtubules (see Supporting Experiments in Supporting Information).

The quantitative correlation between fluorescence lifetime and absolute distance above the surface is given by the model of Chance, Prock, and Silbey (CPS model).⁶ It describes theoretically the reduction of fluorescence lifetime above metal surfaces, allowing for localization of fluorescent molecules with nanometer precision. Adopting this model to our experimental geometry, particularly accounting for an even fluorophore distribution on the contour of the microtubules and the experimentally determined dielectric function of the gold surfaces (see Supporting Discussion), the distance of the fluorescent microtubules from the gold surface (measured from the top of the surface to the bottom of the microtubules, see Figure 1) is 7.5 ± 1.0 nm (s.e.m.) for the avidin-fixed microtubules, 13.3 ± 1.5 nm for the neutravidin-coated and avidin-fixed microtubules, and 26.4 ± 0.9 nm for the kinesin-held microtubules (Figure 2d). These values are expected to directly correspond to the molecular dimensions of the microtubule-attached proteins. Hence, we determine the geometrical size of avidin (molecular weight 66–69 kDa) to about 7.5 ± 1.0 nm (s.e.m.), well in agreement with the size of its tetrameric crystal structure of 4.2 nm \times 7.9 nm \times 7.2 nm.¹¹ We determine the size of neutravidin to be 5.8 ± 1.8 nm, given by the difference between the measurements in panels a and b of Figure 2. Neutravidin is the deglycosylated version of avidin with a molecular weight of about 60 kDa explaining the slightly smaller size compared to avidin. The distance that kinesin-1 holds the microtubules away from the surface is 26.4 ± 0.9

nm in our measurements. This value, which is much shorter than the kinesin-1 contour length of about 60 nm,⁵ is similar to previously described FLIC measurements (15.2 nm).⁵ This indicates a high flexibility of the stalk domain of the kinesin-1. The difference between FLIM and FLIC measurements most likely originates from the different surfaces used in both techniques: in the FLIM approach kinesin-1 motors are coupled to a gold surface, whereas in the FLIC approach the motor proteins are attached to silica surfaces.

Finally, we sensitively visualize local changes in the axial distance along individual microtubules. Therefore, we reconstitute fluorescently labeled microtubules, where the center (but not the ends) is biotinylated¹² (Figure 3). After incubation in a neutravidin solution, these microtubules are avidin-fixed to the gold surface. The center, which binds neutravidin, can clearly be identified as elevated in the lifetime image. For the depicted microtubule, the average lifetimes of the center and end regions are 1.34 ± 0.13 ns (s.d.) and 0.97 ± 0.08 ns (s.d.), respectively. This corresponds to distances of 15.8 ± 2.5 nm (s.d.) and 8.7 ± 1.0 nm (s.d.), yielding a height difference of 7.1 ± 2.7 nm (s.d.). This example demonstrates that the technique is capable of picking up minute height differences even from a single experiment. The precision of these measurements can be increased by averaging over several experiments. When investigating the results from six individual microtubules, we obtain distances of 14.5 ± 0.7 nm (s.e.m.) and 8.6 ± 0.2 nm (s.e.m.) for the center and ends, respectively. The associated height difference of 5.9 ± 0.7 nm (s.e.m.) is in good agreement with the size of the neutravidin molecules of 5.8 ± 1.8 nm (s.e.m.) determined above.

The exactness of our technique is given by the accuracy inherent to the technique and the precision of the individual measurements. For our setup, we have determined the accuracy of the lifetime measurements to ± 0.15 ns (see Supporting Discussion in Supporting Information), which converts into an error in axial distance of about ± 3 nm. This

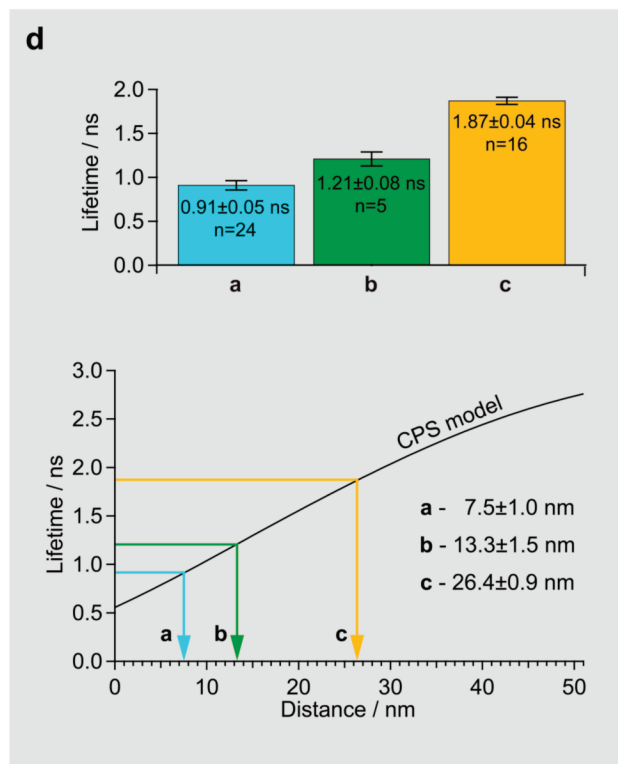
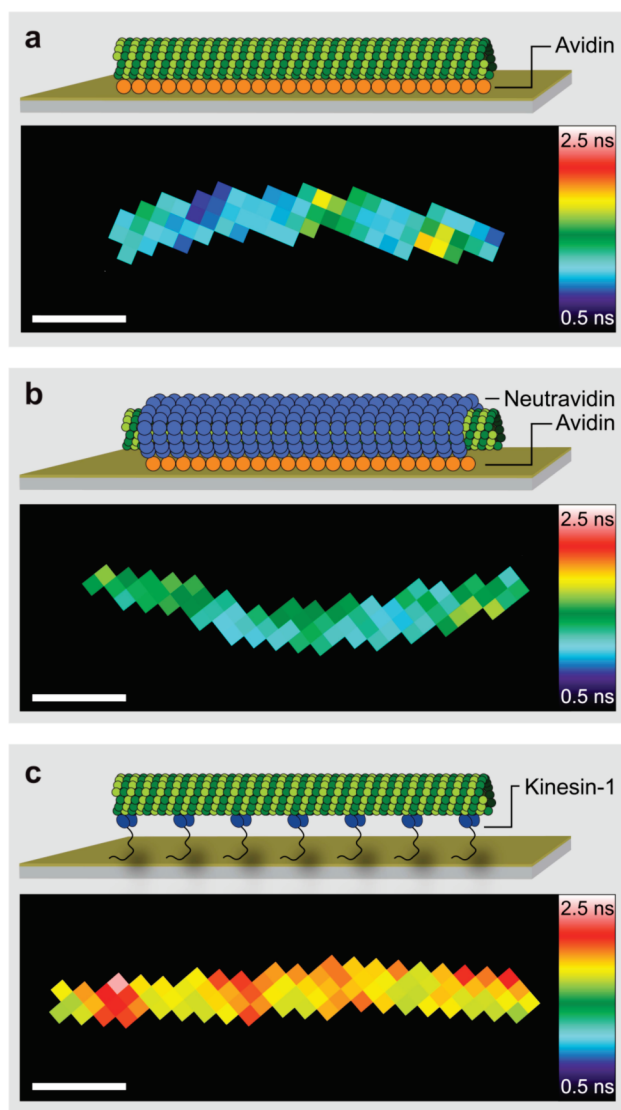


FIGURE 2. Influence of various spacer molecules on fluorescence lifetime and determination of axial distance. (a–c) Microtubules are elevated to different axial positions above a gold surface by avidin (a), neutravidin and avidin (b), or kinesin-1 (c). Shown are experimental schematics and corresponding lifetime images. (d) Measured lifetimes for all experiments (s.e.m.) are converted to absolute distances using the CPS model. Scale bars are 5 μm .

significantly improves the exactness of ± 5 nm achieved with FLIC⁵ or ± 30 nm with TIRF,³ discussed above. The precision is governed by the standard error of the mean (s.e.m.) since the standard deviations of the individual data sets, being less than 0.2 ns, show low variation. This implies a high reproducibility and reliability of the technique.

Our technique offers the intrinsically high exactness of an optical near-field technique combined with an increased robustness compared to techniques such as FLIC and TIRF. In particular, our FLIM approach does not require an in situ calibration and is insensitive to (i) fluorescence intensity variations due to varying labeling ratios (see Table 1 in Supporting Information) and/or bleaching, (ii) spatially inhomogeneous excitation light, and (iii) defocusing (see Supporting Table 1 in Supporting Information). Furthermore, the presented technique is easy to implement on any fluores-

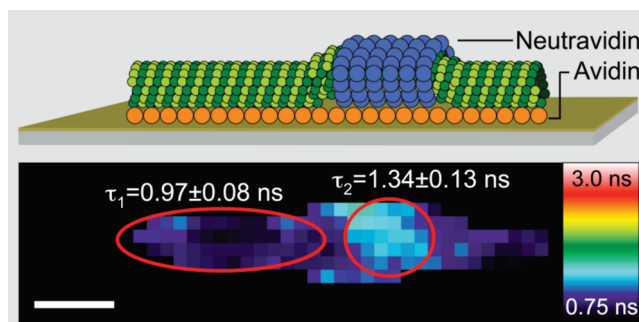


FIGURE 3. Single microtubule elevated to different heights. Schematic and fluorescence lifetime image of a microtubule partially coated with neutravidin. The change in axial distance between the coated and the uncoated part is clearly revealed by different lifetimes. Scale bar is 5 μm .

cence lifetime imaging microscope. When fluorescently labeled microtubules are used as probes, our technique can provide information about the geometrical size, and therefore the conformation, of biomolecules. As demonstrated by our experiments, these measurements are not limited to proteins that naturally bind to microtubules. Rather, any biomolecule can be linked to microtubules via chemical cross-linkers, antibodies, or aptamers. This underlines the versatile use of microtubules for nanotechnology as presented in other studies.^{7,13,14}

We therefore expect the presented technique for molecular measurements to become a versatile tool in fluorescence microscopy and, applied in combination with fluorescent microtubules as probes, to be an important technique for nanobiotechnology.

Acknowledgment. The authors thank Alla Synytska, Brian Ashall, and Corina Bräuer for technical support, Zdenek Petrášek, Frank Cichos, Till Korten, and Gero Fink for helpful discussions, and Chris Gell and Bert Nitzsche for comments on the manuscript. This work was supported by the German Federal Ministry of Education and Research (03N8712), the German Research Foundation (DFG DI 1226/3 and DFG EN 297/12-1), and the Max-Planck-Society.

Supporting Information Available. Supporting methods (microtubule preparation, microtubule assays, experimental

setup and data acquisition), supporting discussion (data analysis, modeling), and supporting experiments (dielectric function of the gold films used, control experiments, determination of the quantum yield of Alexa Fluor 488 labeled microtubules). This material is free of charge via the Internet at <http://pubs.acs.org>.

REFERENCES AND NOTES

- (1) Hell, S. W. *Nat. Methods* **2009**, *6*, 24–32.
- (2) Axelrod, D.; Thompson, N. L.; Burghardt, T. P. *J. Microsc.* **1983**, *129*, 19–28.
- (3) Steyer, J. A.; Almers, W. *Biophys. J.* **1999**, *76*, 2262–2271.
- (4) Braun, D.; Fromherz, P. *Appl. Phys. A: Mater. Sci. Process.* **1997**, *65*, 341–348.
- (5) Kerssemakers, J.; Howard, J.; Hess, H.; Diez, S. *Proc. Natl. Acad. Sci. U.S.A.* **2006**, *103*, 15812–15817.
- (6) Chance, R. R.; Prock, A.; Silbey, R. *Adv. Chem. Phys.* **1978**, *XXXVII*, 1–65.
- (7) Gell, C.; Berndt, M.; Enderlein, J.; Diez, S. *J. Microsc.* **2009**, *234*, 38–46.
- (8) Schliwa, M. *The cytoskeleton, an introductory survey*; Springer-Verlag: Wien and New York, 1986; Vol. 13; pp 1–326.
- (9) Howard, J.; Hyman, A. A. *Methods Cell Biol.* **1993**, *39*, 105–113.
- (10) Ray, S.; Meyhofer, E.; Milligan, R. A.; Howard, J. *J. Cell Biol.* **1993**, *121*, 1083–1093.
- (11) Maatta, J. A. E.; Airene, T. T.; Nordlund, H. R.; Janis, J.; Paldanius, T. A.; Vainiotalo, P.; Johnson, M. S.; Kulomaa, M. S.; Hytonen, V. R. *ChemBioChem* **2008**, *9*, 1124–1135.
- (12) Hyman, A. A. *J. Cell Sci.* **1991**, 125–127.
- (13) Kerssemakers, J.; Ionov, L.; Queitsch, U.; Luna, S.; Hess, H.; Diez, S. *Small* **2009**, *5*, 1732–1737.
- (14) Hess, H.; Clemmens, J.; Howard, J.; Vogel, V. *Nano Lett.* **2002**, *2*, 113–116.